Short Range Order Effects on EPR Frequencies and Magnetic Anisotropy in Heisenberg Linear Chain Antiferromagnets.

by

Kazukiyo Nagata

Institute for Solid State Physics, University of Tokyo,

Roppongi, Minato-ku, Tokyo

(1971)

TABLE OF CONTENTS

ABSTRACT

This paper represents the first successful comparison between experimental results and exact solutions for a simplified phase-transition problem in the presence of a finite magnetic field.

Changes in the position of paramagnetic absorption lines in two typical one-dimensional Heisenberg antiferromagnets, $CsMnCl_3 2H_2O$ and $(CH_3)_4NMnCl_3$, were investigated theoretically and experimentally in the short-range-ordered spin state. The present theory with the classical spin model properly predicts the magnitude and temperature dependence of the shift of resonant field for both crystals. The shift of resonance lines observed for $CsMnCl_3 2H_2O$ can be explained by taking account only of the dipolar term as an anisotropy term. For $(CH_3)_4NMnCl_3$, however, since the single-ion anisotropy is considerably larger, the effect of the D-term has to be taken into account in the explanation of the temperature variation of resonant field.

Torque measurements were done in order to investigate the anisotropy in the paramagnetic susceptibility of $CsMnCl_3 2H_2O$ and the results are compared with the theoretical predictions based on the classical spin model including only a small dipolar term as an anisotropy term. The agreement is satisfactory.

The results of the present work are remarkable especially when one considers the tremendous labor involved in the corresponding problem for two- or three-dimensional systems.

§1. Introduction

Much of the theoretical[1] and experimental[2] studies of the critical phenomena by means of the electron paramagnetic resonance in an antiferromagnet has been related to the line width which, when the critical point is approached, increases anomalously because of the divergent nature of the random torque. On the other hand, few studies[3)~6)] of the temperature dependence of the position of the resonance line in the vicinity of the Néel temperature have been reported. The position of the paramagnetic resonance lines in a magnetically concentrated salt may shift with decreasing temperature by the effect of the short range order in the spin system as well as the effect of the bulk magnetization. For general three-dimensional systems, it does not seem possible at the present stage to discuss quantitatively the effect of the short range order on the resonance position, because it requires the knowledge of the correlation functions in the presence of a finite magnetic field.

However, there is a couple of cases where such correlation functions can explicitly be calculated as a function of temperature and the quantitative discussion of the short-range-order effects may then be possible. One of the exactly soluble cases is a one-dimensional system with Heisenberg Hamiltonian. As Fisher[7] firstly point out, the Heisenberg linear chain problem with zero external field becomes exactly soluble in the (classical) limit of infinite spin. Recently it was found that this class-

ical Heisenberg model properly predicted some of magnetic behaviors of such actual systems as $CsMnCl_3 2H_2O$[8] and $(CH_3)_4NMnCl_3$[9] (hereafter denoted as TMMC). Accordingly, it can be naturally expected that, if we restrict ourselves to such a Heisenberg linear chain antiferromagnet, the temperature variation of the resonance position in the short-range-ordered spin state may be described quantitatively in terms of the classical spin model. In the present thesis, the theoretical and experimental results on the paramagnetic resonance in $CsMnCl_3 2H_2O$ and TMMC will be given as well as the result on the magnetic anisotropy in $CsMnCl_3 2H_2O$.

Both $CsMnCl_3 2H_2O$[10] and TMMC[11] contain Mn^{2+} ions (S=5/2) as magnetic carrier and belong to a class of substances which may be described as linear chain antiferromagnets. In these materials, from structural reasons, dominant superexchange coupling between Mn^{2+} ions occurs in $-MnCl_n-$ chains which extend in each specified direction of the crystals and are magnetically insulated from each other by two or more intervening atoms. The thermal and magnetic properties of the two antiferromagnets have been actually found to be consistent with the expectation based on Fisher's exact solution[7] of the classical one-dimensional Heisenberg antiferromagnets, above about 10 K for $CsMnCl_3 2H_2O$[8),12] and 1.1 K for TMMC[9),13] respectively. The two materials, therefore, are much favourable to study the static and dynamic behaviors of a one-dimensional system with considerably lone-range one-dimensional

correlations in the absence of the three-dimensional effects.

As reported in the previous short note[5], Tazuke and the author discovered firstly for $CsMnCl_3 2H_2O$ anomalously large shfits of the paramagnetic resonance lines when the temperature was reduced and the Néel point was approached. Furthermore, a similar temperature dependence of the resonance positions was recently observed for TMMC by them. The shifts of both materials have a uniaxial symmetry referred to the directions of chains and their amplitudes seem to reflect the development of intrachain spin correlations. Besides the torque measurement performed on $CsMnCl_3 2H_2O$ by the author revealed that, though the magnetic carrier of this salt is regarded as isotropic in magnetic moment, the anomalously large axial anisotropy appears in the paramagnetic susceptibility in the short-range-ordered spin state. Accordingly, it can be deduced that the magnetic dipole interactions among short-range-ordered spins in the chain may be responsible for the line-shifting mechanism and the enhancement of anisotropy.

The confirmation of the above inference requires the knowledges on the relation between the resonance frequencies or susceptibilities and the correlation functions and on the explicit expressions of the correlation functions in the presence of a finite magnetic field as a function of temperature. Theoretical discussions for these problems are given in next section and the results are compared with our experimental data in section 5. The agreements are excellent, particularly for $CsMnCl_3 2H_2O$. This

work then represents the first successful comparison between experimental results and an exact solution for a simplified phase-transition problem in the presence of a finite magnetic field.

§2. Theory

In a linear chain system consisting of atomic spins coupled with each other by isotropic exchange interaction, a most important source of magnetic anisotropy energy with uniaxial symmetry referred to the direction of chain (hereafter denoted as the z-direction) is the purely magnetic dipolar interactions between spins given by

$$\sum_{ij} \frac{g^2\mu_B^2}{r_{ij}^3} (\vec{S}_i \cdot \vec{S}_j - 3S_i^z S_j^z). \tag{1}$$

For a one-dimensional lattice, such a dipolar sum converges rapidly. Then one can approximate Eq. (1) by an interaction between the nearest neighbors, that is,

$$\frac{g^2\mu_B^2}{r_0^3} \sum_{j=1} (\vec{S}_j \cdot \vec{S}_{j-1} - 3S_j^z S_{j-1}^z), \tag{2}$$

where r_0 is the nearest-neighbor separation in the chain. Accordingly the Hamiltonian for such a linear chain system of N+1 atoms of spin S in an external magnetic field H can be written as

$$\mathcal{H} = -2J(1+\alpha) \sum_{j=1}^{N} \vec{S}_j \cdot \vec{S}_{j-1} + 6J\alpha \sum_{j=1}^{N} S_j^z S_{j-1}^z - g\mu_B \sum_{j=0}^{N} \vec{S}_j \cdot \vec{H} \tag{3}$$

with

$$\alpha = -1/(2J)(g^2\mu_B^2/r_0^3). \tag{4}$$

In the following subsections, the electron paramagnetic

resonance frequencies for the linear chain system will be considered for the case where an external magnetic field is sufficiently strong as compared with the dipolar interaction between adjacent spins and the temperature variation of the shift of the effective g-values will be calculated explicitly in the classical limit of infinite spin. Continuously the anisotropy in the paramagnetic susceptibility for the one-dimensional system will be quantitatively described according to the classical spin model and the relation between the shift of resonance lines and the anisotropic susceptibility will be discussed.

A) Paramagnetic Resonance Frequencies

It may be pictured for paramagnetic resonances that the bulk magnetic moment[14] of entire specimen makes a precessional motion about the static magnetic field at an angle which depends on the amplitude of the r-f field, the proximity to resonance, and damping factors. Such motion of the total spin $\vec{S}$ is determined by the quantum mechanical equation of motion,

$$i\hbar(d\vec{S}/dt) = [\vec{S},\mathcal{H}], \tag{5}$$

where $\mathcal{H}$ is a Hamiltonian as in Eq. (3). We shall here consider the statistical average of the commutator, $[S^-,\dot{S}^+]$. It comes out from Eq. (5) to be

$$i\hbar\langle[S^-,\dot{S}^+]\rangle = \langle[S^-,[S^+,\mathcal{H}]]\rangle, \tag{6}$$

where we denote the thermal average by $\langle \quad \rangle$. If we neglect the effect of relaxation on the resonance frequency and assume that S^+ and S^- are good normal modes, the time dependence of each transverse component of $\vec{S}$ can be taken to be proportional to $\exp(i\omega t)$, that is,

$$\dot{S}^+ = i\omega S^+. \tag{7}$$

The physical plausibility of Eq. (7) may be certified for the case where the operating frequency is sufficiently larger than the dipolar frequency. This situation could be realized in the present experiments. By putting Eq. (7) into Eq. (6), the eigen-frequency can be obtained as

$$\hbar\omega = \frac{\langle [S^-,[S^+,\mathcal{H}]] \rangle}{2\langle S^z \rangle} . \tag{8}$$

As is seen in Appendix A, this approach to the frequency corresponds to the calculation of the first moment of $Im\chi(\omega)$, the imaginary part of the high frequency magnetic susceptibility. Moreover, the expression (8) can also be derived from the density matrix approach by Kanamori and Tachiki[15].

Let us consider the case of a linear chain system described by Hamiltonian (3) with an external field H along the z-direction. For this case, the x- and y-directions are equivalent because of uniaxial symmetry. By a simple calculation one can obtain from the relation (8) the resonance frequency as

$$\hbar\omega_{\parallel} = g\mu_B H - \frac{12J\alpha N\langle S_m^z S_{m+1}^z - S_m^x S_{m+1}^x\rangle_{H\parallel z}}{\langle S^z\rangle_{H\parallel z}} . \qquad (9)$$

For the case where an external field is applied parallel to the x-direction, the analogous expression for the resonance frequency is

$$\hbar\omega_{\perp} = [g\mu_B H(g\mu_B H - \frac{12J\alpha N\langle S_m^z S_{m+1}^z - S_m^x S_{m+1}^x\rangle_{H\parallel x}}{\langle S^x\rangle_{H\parallel x}})]^{1/2} \qquad (10)$$

Since we have confined ourselves to the case of small dipolar interactions, Eq. (10) can be reduced to

$$\hbar\omega_{\perp} = g\mu_B H + \frac{6J\alpha N\langle S_m^x S_{m+1}^x - S_m^z S_{m+1}^z\rangle_{H\parallel x}}{\langle S^x\rangle_{H\ x}} . \qquad (11)$$

$\langle S^z\rangle$ in Eq. (9) and $\langle S^x\rangle$ in Eq. (11) are related to the magnetic susceptibilities by

$$\langle S^z\rangle_{H\parallel z} = (\chi_{\parallel} H)/(g\mu_B)$$

and

$$\langle S^x\rangle_{H\parallel x} = (\chi_{\perp} H)/(g\mu_B), \qquad (12)$$

respectively.

For the case where the short-range-order effects are negligible, the average $\langle S_m^z S_{m+1}^z - S_m^x S_{m+1}^x\rangle$ can be replaced by $\langle S_m^z\rangle^2$ for $H\parallel z$ and $-\langle S_m^x\rangle^2$ for $H\parallel x$, and then Eq. (9) and (11)

reduce to

$$\hbar\omega_{\parallel} = g\mu_B H\left(1 - \frac{12J\alpha\chi_{\parallel}}{Ng^2\mu_B^2}\right) \tag{13}$$

and

$$\hbar\omega_{\perp} = g\mu_B H\left(1 + \frac{6J\alpha\chi_{\perp}}{Ng^2\mu_B^2}\right). \tag{14}$$

Accordingly the resonance frequencies are temperature dependent only through the temperature dependence of the magnetic susceptibilities. This does not explain our experimental results, indicating the importance of the short-range-order effects.

In the present problem, it is essential to calculate the correlation function $\langle S_m^z S_{m+1}^z - S_m^x S_{m+1}^x \rangle$ as a function of temperature taking full account of the short-range-order effect. Several years ago, Fisher[7] pointed out that the purely isotropic Heisenberg chain problem became exactly soluble for H=0 in the classical limit of infinite spin. He obtained compact closed expressions for the pair correlation functions of such a system. However, his result for H=0 is not directly applicable to our problem; the correlation function $\langle S_m^z S_{m+1}^z - S_m^x S_{m+1}^x \rangle$ vanishes. Then we shall attempt to extend the calculation to the case of finite H and small anisotropy effects.

To go over to the classical limit, the quantum-mechanical spin operators in the Hamiltonian (3) have to be replaced with classical vectors. Following Fisher's procedure, we shall

introduce unit vector operators $\vec{s}_j = S(S+1)^{-1/2}\vec{S}_j$ associated with the j-th spin and treat them as classical vectors. The correction for large finit S with respect to the classical results for $S=\infty$ is of order $1/S^2$ [7]. The resulting classical Hamiltonian for a small α can be expressed by

$$\mathcal{H} = -2JS(S+1)\sum_{j=1}^{N}\vec{s}_j\cdot\vec{s}_{j-1} + 6JS(S+1)\alpha\sum_{j=1}^{N}s_j^{z}s_{j-1}^{z} - g\mu_B[S(S+1)]^{1/2}\sum_{j=0}^{N}\vec{s}_j\cdot\vec{H}. \tag{15}$$

For the simple case with purely isotropic Heisenberg coupling and zero external field, the pair correlation functions have been obtained in the classical limit by Fisher as follows:

$$\langle s_m^{z}s_{m+l}^{z}\rangle_0 = (1/3)\{u(K)\}^{|l|}, \tag{16}$$

where

$$K = \frac{2JS(S+1)}{kT} \tag{17}$$

and

$$u(K) = \coth K - 1/K. \tag{18}$$

If we restrict ourselves to the physical condition that the dipolar energy is sufficiently smaller than the Zeeman energy, we can neglect the effect of dipolar interactions on the short range order and treat the Zeeman terms as a perturbing Hamiltonian.

Using the Hamiltonian

$$\mathcal{H} = -2JS(S+1) \sum_{j=1}^{N} \vec{s}_j \cdot \vec{s}_{j-1} - g\mu_B [S(S+1)]^{1/2} \sum_{j=0}^{N} \vec{s}_j \cdot \vec{H}, \tag{19}$$

the correlation function $\langle S_m^z S_{m+1}^z - S_m^x S_{m+1}^x \rangle$ in the presence of a small external field parallel to the z-direction can be expressed in terms of the higher order spin correlations in zero field. To the second order in H, we have

$$\langle S_m^z S_{m+1}^z - S_m^x S_{m+1}^x \rangle_{H \| z} = (1/2)[g\mu\, HS(S+1)/(kT)]^2$$

$$\times \sum_{i=0}^{N} \sum_{j=0}^{N} \langle (s_m^z s_{m+1}^z - s_m^x s_{m+1}^x) s_i\, s_j \rangle_0 . \tag{20}$$

For the case with a field parallel to the x-direction, the analogous expression can be obtained only by interchanging $(s_m^z s_{m+1}^z)$ with $(s_m^x s_{m+1}^x)$. Then we have

$$\langle S_m^z S_{m+1}^z - S_m^x S_{m+1}^x \rangle_{H \| z} = -\langle S_m^z S_{m+1}^z - S_m^z S_{m+1}^z \rangle_{H \| x} . \tag{21}$$

The summation in the right-hand side of Eq. (20) are given in Appendix B for a large system and only the results are presented here:

$$\sum_{i=0}^{N} \sum_{j=0}^{N} \langle (s_m^z s_{m+1}^z - s_m^x s_{m+1}^x) s_i^z s_j^z \rangle_0$$

$$= \frac{2}{15} \frac{(2-u/K)}{(1-u)^2} + \frac{4K}{45} \frac{(1+u)}{(1-u)} . \tag{22}$$

The magnetic susceptibilities, which appear in the resonance conditions (9) and (11) through the relations (12), can be approximately substituted by Fisher's expression for zero field:

$$\chi = \frac{Ng^2\mu_B{}^2 S(S+1)}{3kT} \frac{(1+u)}{(1-u)} , \tag{23}$$

which is easily derived from the relation (16). Accordingly, the frequency-shift terms in Eq. (9) and (11) can now be expressed explicitly as a function of temperature. For J<0, one obtains

$$\Delta\hbar\omega_{\parallel} = \frac{12|J|\alpha N\langle S_m{}^z S_{m+1}{}^z - S_m{}^x S_{m+1}{}^x\rangle_{H\parallel z}}{\langle S^z\rangle_{H\parallel z}}$$

$$= 12\alpha g\mu_B H\, F(x) \tag{24}$$

and

$$\Delta\hbar\omega_{\perp} = -(1/2)\Delta\hbar\omega_{\parallel} , \tag{25}$$

where

$$F(x) = \frac{1}{10x}\left(\frac{2+ux}{1-u^2} - \frac{2}{3x}\right) \tag{26}$$

and

$$x = \frac{kT}{2|J|S(S+1)} = -1/K. \tag{27}$$

The numerical results of F(x) are shown in Fig. 1(a). At low temperatures F(x) is asymptotically proportional to T^{-2}, while at

high temperatures it is proportional to T^{-1}, being consistent with Eq. (13) and (14).

B) Magnetic Susceptibility

As is well known, the magnetic susceptibility for a weak magnetic field parallel to the γ-direction can be calculated from the fluctuation relation

$$\chi(T) = \frac{g^2\mu_B{}^2}{kT} \sum_{i=0}^{N} \sum_{j=0}^{N} \langle S_i{}^{\gamma} S_j{}^{\gamma} \rangle, \tag{28}$$

when diamagnetic effects are neglected. Going to the same classical limit employed in the preceding subsection, we write Eq. (28) as

$$\chi(T) = \frac{g^2\mu_B{}^2 S(S+1)}{kT} \sum_{i=0}^{N} \sum_{j=0}^{N} \langle s_i{}^{\gamma} s_j{}^{\gamma} \rangle. \tag{29}$$

We shall now calculate the pair correlation functions in Eq. (29) by a perturbation procedure, considering the dipolar and Zeeman terms as a perturbing Hamiltonian. Using the total Hamiltonian (15), the resulting expression for the susceptibility for H$\parallel$z in terms of unperturbed spin-correlation functions becomes, to first order in Jα,

$$\chi_{\parallel} = \frac{g^2\mu_B{}^2 S(S+1)}{kT}\{\sum_{i=0}^{N}\sum_{j=0}^{N}\langle s_i{}^z s_j{}^z\rangle + \frac{6|J|S(S+1)\alpha}{kT}\sum_{i=0}^{N}\sum_{j=0}^{N}\sum_{k=1}^{N}$$

$$\times [\langle s_i{}^z s_j{}^z (s_k{}^z s_{k-1}{}^z)\rangle_0 - \langle s_i{}^z s_j{}^z\rangle_0 \langle s_k{}^z s_{k-1}{}^z\rangle_0]\}, \qquad (30)$$

where $\langle\ \ \rangle_0$ refers to an average with respect to the unperturbed Hamiltonian. The analogous expression for $\chi_{\perp}$ differs only in the substitution of $(s_k{}^x s_{k-1}{}^x)$ for $(s_k{}^z s_{k-1}{}^z)$. Consequently the anisotropy in the susceptibility turns out to be written in the following simple form:

$$\chi_{\parallel} - \chi_{\perp} = \frac{6|J|\alpha[g\mu_B S(S+1)]^2}{(kT)^2}\sum_{i=0}^{N}\sum_{j=0}^{N}\sum_{k=1}^{N}$$

$$\times \langle s_i{}^z s_j{}^z (s_k{}^z s_{k-1}{}^z - s_k{}^x s_{k-1}{}^x)\rangle_0. \qquad (31)$$

The summations in the right-hand side of Eq. (31) has been given in Eq. (22). Putting the result into Eq. (31),

$$\chi_{\parallel} - \chi_{\perp} = \frac{N|J|\alpha[g\mu_B S(S+1)]^2}{(kT)^2}\ \frac{4}{5}\{\frac{2-u/K}{(1-u)^2} + \frac{2K}{3}\frac{1+u}{1-u}\}$$

$$= N\alpha^2 r_0{}^3\ P(x), \qquad (32)$$

where

$$P(x) = \frac{2}{5x^2}\{\frac{2+ux}{(1-u)^2} - \frac{2}{3x}\frac{(1+u)}{(1-u)}\}, \qquad (33)$$

which has the high-temperature expansion,

$$P(x) = (2/3)x^{-2} - (32/45)x^{-3} + \ldots \tag{34}$$

and the low-temperature expansion,

$$P(x) = (1/15)x^{-2} + (1/30)x^{-1} + \ldots \tag{35}$$

The numerical results of P(x) are shown in Fig. 1(b). The anisotropy given by Eq. (32) then vanishes at high temperatures and increases monotonously with decreasing temperature.

C) Effects of the Single Ion Anisotropy Energy

In this paragraph, we shall consider briefly the effects of the one-ion type anisotropy energy on the paramagnetic resonance frequencies and the anisotropy in the susceptibility. If the crystalline environment of each magnetic ion has axial symmetry referred to the chain direction, single ion energy of the form $D(S_j^z)^2$ may does play an important role in the shift of the resonance frequencies and the anisotropy in the magnetic susceptibility. The Hamiltonian for a linear chain system with such uniaxial single-ion anisotropy has the following additional term to Eq. (3):

$$\mathcal{H}_D = D \sum_{j=0}^{N} (S_j^z)^2, \tag{36}$$

where D is the same constant for each of N+1 atoms in the chain. The effects of such D-term on the g-shift and the anisotropy can be evaluated in a similar way to the dipolar term.

For the paramagnetic resonance frequencies, we obtain the correction of the D-term as

$$(\Delta\hbar\omega_{\parallel})_D = \frac{-2ND\langle (S_m^z)^2 - (S_m^x)^2\rangle_{H\parallel z}}{\langle S^z\rangle_{H\parallel z}} \tag{37}$$

and

$$(\Delta\hbar\omega_{\perp})_D = \frac{-ND\langle (S_m^z)^2 - (S_m^x)^2\rangle_{H\parallel x}}{\langle S^x\rangle_{H\parallel x}} . \tag{38}$$

As long as we concern the physical condition that the Zeeman energy is sufficiently larger than the axial anisotropy energy,

$$\langle (S_m^z)^2 - (S_m^x)^2\rangle_{H\parallel z} = - \langle (S_m^z)^2 - (S_m^x)^2\rangle_{H\parallel x}. \tag{39}$$

The thermal average, $\langle (S_m^z)^2 - (S_m^x)^2\rangle$, can also be calculated by the classical spin model with a classical perturbing Hamiltonian

$$\mathcal{H}_D = DS(S+1) \sum_{j=0}^{N} (s_j^z)^2, \tag{40}$$

which are given in Appendix C. Putting the result into Eq. (37) and (38), we obtain

$$(\Delta\hbar\omega_{\parallel})_D = -(DN/\langle S^z\rangle_{H\parallel z})\left[\frac{g\mu_B S(S+1)H}{kT}\right]^2$$

$$\times \sum_{i=0}^{N}\sum_{j=0}^{N}\langle\{(s_m{}^z)^2 - (s_m{}^x)^2\}s_i{}^z s_j{}^z\rangle_0$$

$$= -(D/|J|)g\mu_B H\ G(x) \tag{41}$$

and

$$(\Delta\hbar\omega_{\perp})_D = -(1/2)(\Delta\hbar\omega_{\parallel})_D, \tag{42}$$

where

$$G(x) = \frac{1}{5x}\left\{\frac{2u}{1-u^2} - 1 - \frac{2}{3ux}\right\}. \tag{43}$$

The additional anisotropy in the susceptibility, resulting from the D-term, can be obtain in the same classical model as follows:

$$(\chi_{\parallel} - \chi_{\perp})_D = -\frac{D[g\mu_B S(S+1)]^2}{(kT)^2}$$

$$\times \sum_{i=0}^{N}\sum_{j=0}^{N}\sum_{k=0}^{N}\langle s_i{}^z s_j{}^z\{(s_k{}^z)^2 - (s_k{}^x)^2\}\rangle_0$$

$$= -N\alpha r_0{}^3\ D/(2|J|)\ Q(x), \tag{44}$$

where

$$Q(x) = \frac{2}{15x^2}\left\{\frac{(1+u)(1+v)}{(1-u)(1-v)} + \frac{2u}{(1-u)^2}\right\} \tag{45}$$

and

$$v = 1 + 3ux. \tag{46}$$

In contrast to the monotonous temperature-variation of F(x) or P(x), both G(x) and Q(x) pass through a round maximum and turn into negative values at a temperature of $(|J|/k)S(S+1)$, when the temperature is reduced. The negative values of G(x) or Q(x) suggest that it is favorable for the spins to tend towards directions perpendicular to the external magnetic field below the temperature of $(|J|/k)S(S+1)$. The numerical results of G(x) and Q(x) are shown in Fig. 2(a) and 2(b), respectively.

D) Expressions of the g-Shifts in Terms of $\chi_{\parallel}$ and $\chi_{\perp}$

As was mensioned in the preceding paragraphs, the shift of the effective g-values in the paramagnetic resonance for a classical Heisenberg linear chain system with small dipolar- and D-terms can be expressed as follows:

$$\Delta g_{\parallel} = (g/\chi_{\parallel})\left[\frac{g\mu_B S(S+1)}{kT}\right]^2$$

$$\times N \sum_{i=0}^{N} \sum_{j=0}^{N} \{6|J|\alpha\langle(s_m^z s_{m+1}^z - s_m^x s_{m+1}^x)s_i^z s_j^z\rangle_0$$

$$- D\langle[(s_m^z)^2 - (s_m^x)^2]s_i^z s_j^z\rangle_0\}, \tag{47}$$

and

$$\Delta g_{\perp} = -(1/2)(\chi_{\parallel}/\chi_{\perp})\Delta g_{\parallel}. \tag{48}$$

with the use of the relations (31) and (44), these expressions become following compact forms:

$$\Delta g_{\parallel}/g = (\chi_{\parallel} - \chi_{\perp})/\chi_{\parallel},$$

$$\Delta g_{\perp}/g = (\chi_{\perp} - \chi_{\parallel})/(2\chi_{\perp}). \tag{49}$$

It should be noticed that, in the above calculations of the resonance frequencies and the susceptibilities, we neglected the higher terms than the quadratic terms in $J\alpha$ or D. It then seems that Eq. (49) hold only for the case where the operating frequency is sufficiently larger than the axial anisotropy frequency of the relevant magnetic system.

§3. Magnetical One-Dimensionality of $CsMnCl_3 2H_2O$ and TMMC

The first evidence of linear chain behavior in $CsMnCl_3 2H_2O$ was given by the susceptibility measurement of Friedberg et al.[8] They found that, when the temperature decreased, a rounded maximum in the susceptibility was observed near 25 K, as expected for a spin system consisting of independent linear chains of Mn^{2+} ions coupled by antiferromagnetic isotropic exchange with J=-3.0 K. This magnetical one-dimensionality in $CsMnCl_3 2H_2O$ can be understood from the crystallographic structure determined by Jensen et al.[10] This material forms orthorhombic crystals characterized by the space group Pcca-D_{2h}^8, with a=9.060 A, b=7.285 A, and c=11.455 A, containing four formula units in a unit cell. A projection of the structure on the (001) plane is shown in Fig. 3. This orthorhombic structure may be regarded as a set of chains parallel to the a-axis. Each Mn^{2+} ion is surrounded by a highly distorted octahedron of four Cl^- ions and two oxygen atoms. Since neighboring octahedra along the a-axis share a Cl^- ion as a common ligand, dominant superexchange coupling of Mn^{2+} ions occurs only in a chain of $-Cl^--Mn^{2+}-Cl^--Mn^{2+}-$ along the a-axis, whereas the chains are in relative isolation from one another in the perpendicular directions. Recently neutron diffraction study[12] has revealed that substantial intrachain spin correlations develop well between 10 and 40 K.

$CsMnCl_3 2H_2O$ exhibits three-dimensional antiferromagnetic long-range ordering at 4.89 K[16] and the magnetic behaviors below

the Neel point can be understood as a usual three-dimensional antiferromagnet[12),17)~20)].

Recent magnetic studies of TMMC[13)] have indicated that this salt is a more ideal one-dimensional antiferromagnet than $CsMnCl_3 2H_2O$. The crystal structure[11)] of TMMC belongs to the space group $P6_3/m\text{-}C_{6h}^2$, with a=9.151 A and c=6.494 A. Mn^{2+} ions occupy special positions at (000) and (001/2) and are surrounded by trigonally distorted octahedra of Cl^- ions. A projection of the structure on the (001) plane is shown in Fig. 4(a). This structure may be regarded as a hexagonal array of antiferromagnetic $-MnCl_3-$ chains along the c-axis which are shown in Fig. 4(b). Because these $-MnCl_3-$ chains are magnetically insulated from each other by intervening large $[N(CH_3)_4]^+$ ions, three-dimensional long-range order in this antiferromagnet is established at very low temperature as 0.84 K through the action of the weak inter-chain dipolar interactions, although the expected broad maximum in the susceptibility is observed near 55 K[13)]. The intrachain spin correlations[9)] have also been directly observed above 1.1 K in the quasielastic neutron experiments of TMMC.

§4. Experimental Procedure

A) Preparation of the Specimens

$CsMnCl_3 2H_2O$ crystals used in the present experiment were grown by slow evaporation of saturated aqueous solutions of CsCl and $MnCl_2 4H_2O$ at about 30 C. With care it was possible to obtain pink single crystals up to $10 \times 5 \times 1$ mm^3 in size. These crystals have a (001) preferred growth plane and exhibit well developed (100) type faces. Then the specimens can be easily oriented from the morphology.

Crystals of TMMC were grown by slowly evaporating a nearly 1-mole HCl solution of tetramethylammonium chloride and $MnCl_2 4H_2O$. The rose-colored crystals obtained are in the form of slender hexagonal prisms with a preferred growth axis parallel to the chain direction [001]. To prevent deliquescence which brings frequently undesirable impurity-signal besides a foundamental line, the specimens had to be coated with pure clock oil.

B) ESRMeasurement

Usual experimental apparatus and techniques for the microwave reflection method were used in the range of 34 GHz to observe the paramagnetic resonance absorptions in $CsMnCl_3 2H_2O$ and TMMC. The large line-width up to 3 kOe for these materials required the cylindrical cavity spectrometer with variable coupling iris the several samples with $1 \sim 0.1$ mm^3 in size. The sample magnetiza-

tion effects were not found important except for high temperature regions in the present work, because the observed-changes of resonance positions were too large to correct for such effects.

The temperature of the sample mounted on the bottom of the resonant cavity was controlled by the following procedure. The cavity connected to the end of the Cu-Ni wave guide was placed inside of double Dewar vessels above the level of liquid He^4 and was cooled by the flow of the cooled He^4 gas. Two heaters, one immersed in the liquid helium and the other placed close to the cavity, could maintain the sample-temperature fluctuation within ± 0.1 K during each run. The temperature measurements were made by using a commercial carbon thermometer below 50 K and AuCo-Cu thermocouple above 50 K.

The crystal orientations were performed by the morphology and were checked by observing the angular dependence of the antiferromagnetic resonance in $CsMnCl_3 2H_2O$ at 1.5 K and the angular dependence of the high temperature line-width in TMMC. It is believed that the crystal orientation usually was better than $\pm 2^o$.

C) Torque Measurement

The magnetic torque caused by the anisotropy in the susceptibility of $CsMnCl_3 2H_2O$ was measured by using the automatic recording type torquemeter. The measuring temperature could

be varied between 1 K and room temperature and the measurable range of the magnitude of the torque was from 1 to 10^4 dyne-cm.

§5. Experimental Results and Discussions

A) Paramagnetic Resonance

a) $CsMnCl_3 2H_2O$

Measurements of the position of the paramagnetic resonance line in $CsMnCl_3 2H_2O$ were made at 34.4 GHz as a function of temperature and orientation. The values of the shift in the resonant filed from the high temperature limit are shown in Fig. 5 for three orientations of the magnetic field (parallel to the orthorhombic a-, b- and c-axis). It is interesting to note that, when the temperature decreases, the resonant field begins to shift with a uniaxial symmetry referred to the chain-direction (a-axis) at the temperature of about $10T_N$ below which the development of intrachain spin correlations has been observed in the neutron diffraction study[12] of this salt. This shift in the resonant field cannot be due to the effect of the sample magnetization, for the susceptibility of $CsMnCl_3 2H_2O$ may be rather regarded to be roughly temperature-independent in the temperature region where the shift could be observed. The previous antiferromagnetic resonance study by the author and Tazuke[17] has concluded that the magnetic anisotropy in this material mainly arises from the purely magnetic dipolar interaction between spins. If the relevant magnetic system can be substantially regarded as a linear chain magnet, such dipolar interaction must have a uniaxial symmetry, particularly, of easy plane type for an antiferromagnet. As will be seen later, the uniaxial anisotropy in this antiferro-

magnet has been confirmed by the torque measurements in the same temperature region as this resonance study. Therefore, the observed results on the shift in the resonant field can be directly compared with Eq. (24) and (25). As is seen in Fig. 5, the agreement is excellent at all temperatures between $2T_N$ and $10T_N$ for the exchange constant of $J=-3.57$ K which was determined by the spin wave spectrum below T_N[12] and the nearest-neighbor separation, $r_0=4.530$ A. So the present theory is a very good description of the temperature dependence of paramagnetic resonance field for such a Heisenberg linear chain system with considerably large spins as this manganese salt.

As reported in the previous note[5], the broadening of paramagnetic resonance line could be observed in the same temperature range as this work. Comparison with Mori's theory[1], however, does not give good agreement. The absorption line shapes seemed to be symmetric and typical Lorentzian at all temperatures of this experiment.

b) TMMC

Analogous measurements were made for single crystals of the one-dimensional antiferromagnet TMMC at 34.9 GHz. Fig. 6 shown the temperature dependence of the position of the resonance line for two orientations of the magnetic field ($H \parallel c$ and $H \perp c$). As is seen in Fig. 6, comparison with Eq. (24) and (25) (solid lines)

for J=-6.3 K[13] and the nearest-neighbor separation of 3.247 A does not give so good agreement as in $CsMnCl_3 2H_2O$.

Most possible mechanism to explain the quantitative disagreement roughly by a factor of 2 is an additional one-ion type anisotropy given by $D \sum_{j=0}^{N} (S_j^z)^2$. Each Mn^{2+} ion in this salt is surrounded by a slightly distorted octahedron of ligands and lies on a three-fold axis parallel to the chain-direction (c-axis) and then the c-axis of the crystal corresponds to the z-direction of the one-ion anisotropy. The effect of such D-term on the resonance frequency-shift was considered in section 2 and the corrections of the D-term have been given by Eq. (41) and (42). The theoretical results indicate that, when the coefficient D is negative, the effects of the d-term and the dipolar term on the resonance frequency are inclined to cancel each other. The dotted lines in Fig. 6 show the corrected values by taking account of the single-ion anisotropy with $D=-0.10\ cm^{-1}$. The quantity $D=-0.10\ cm^{-1}$ measures the splitting in zero field of the Mn^{2+} ion ground state into three Kramers doublets. This value of D inferred from our results is reasonably compared with the value assumed in the optical study of this salt[21].

It is somewhat difficult to discuss the origin of this easy-axis type anisotropy. We shall here only note that the considerably large g-value observed as 2.005 at room temperatures may be related to the uniaxial anisotropy.

B) Anisotropy in the susceptibility

In order to study the anisotropy in the magnetic susceptibility of a Heisenberg linear chain antiferromagnet, the torque measurements were performed for a single crystal of $CsMnCl_3 2H_2O$ at temperatures between 4.2 and 77.3 K by rotating an external magnetic field in the ab- and bc-plane. The observed torque curves are ordinary paramagnetic $\sin 2\phi$ curves for both planes at all temperatures above the Néel point and show that the paramagnetic principal axes coincide with the orthorhombic axes of this crystal. For measurements at a constant temperature, when we plot the amplitudes of the $\sin 2\phi$ curves against H^2, the square of the field strength, the points fall well on a straight line and then from the slope of the line we can obtain the value of the anisotropy of the susceptibility at the temperature. The results are given as a function of temperature in Fig. 7. It is interest to note that the anisotropy in the susceptibility of $CsMnCl_3 2H_2O$ has an essentially uniaxial symmetry referred to the direction of chain (a-axis) above about $2T_N$ and becomes orthorhombic below $2T_N$. This is consistent with the results of neutron diffraction study by Skalyo et al.[12] and can be understood as the reflection of the magnetically effective dimensionality of the system, that is, the uniaxial symmetry above $2T_N$ may result from the substantial intrachain spin correlations and the orthorhombicity below $2T_N$ may be caused by the evolution of three-dimensional magnetic correlations.

We shall here attempt to describe quantitatively the uniaxial anisotropy, $\chi_a - \chi_b$, above about 10 K in terms of the classical spin model discussed in section 2. As is seen from Fig. 3, there is no reason to expect that the single-ion anisotropy of this crystal should have an axial symmetry referred to the a-axis. Accordingly, the most important source of the axial anisotropy is the purely magnetic dipolar interactions between spins given by Eq. (1). Then Eq. (32) can be directly applied to the present problem. Fig. 8 shows the comparison of Eq. (32) with the experimental data, where J and r_0 are taken as -3.57 K and 4.530 A, respectively. As is seen in the figure, the agreement is satisfactory. So the classical spin model, including only a small dipolar term as an anisotropy term, is a good description of the magnitude and temperature variation of the uniaxial magnetic anisotropy in $CsMnCl_3 2H_2O$ as well as in the matter of the g-shift of paramagnetic resonance.

C) Summary of Results

This work reports the first studies of the short-range-order effects on the paramagnetic resonance frequency and the paramagnetic susceptibility. The present theory with the classical spin model properly predicts the magnitude and temperature variation of the shift of paramagnetic resonance lines for both crystals, $CsMnCl_3 2H_2O$ and TMMC, as well as those of the anisotropy

in the susceptibility of $CsMnCl_3 2H_2O$. This is a remarkable result especially when one considers the tremendous labor involved in the corresponding problem for the two and three-dimensional systems.

The shift of resonance lines and the magnetic anisotropy, observed for $CsMnCl_3 2H_2O$, could be explained by taking account only of the dipolar term as an anisotropy term. For TMMC, however, since the single-ion anisotropy is considerably larger, the effect of the D-term had to be taken into account in the analysis of the temperature variation of the resonant field.

The present approach to the calculation of paramagnetic resonance frequencies may be equivalent to that by the method of line moments. When the magnitude of the external magnetic field is comparable with or smaller than the anisotropy field, its validity is lost. For such case, it seems much more complicated to treat the paramagnetic resonance frequency in the whole temperature range above the transition point.

ACKNOWLEDGEMENTS

It is a pleasure to thank Professor M. Date of Osaka University for his many physical insights and encouragement through all the course of this work. I would also like to thank Professors T. Moriya and Y. Tomono as well as Professor Date for valuable discussions concerning some of the problems in this thesis. Thanks are also due to Mr. Y. Tazuke for his cooperation in this work and especially in the ESR measurements. Finally the author wish to thank Dr. K. Tsushima of NHK Broadcasting Sience Research Lab. for the use of some of his equipments.

APPENDIX A:

The n-th moment of a resonance is defined by

$$\mu_n = \int_{-\infty}^{\infty} \omega^n Im\chi^{+-}(\omega)d\omega , \qquad (A-1)$$

where $Im\chi^{+-}(\omega)$ is the imaginary part of the high frequency magnetic susceptibility whose quantum mechanical expression is given by

$$\chi^{+-}(\omega) = [i(g\mu_B)^2/\hbar]\int_{-\infty}^{\infty} dt\ \theta(t)\langle[S^-,S^+(t)]\rangle e^{-i\omega t} \qquad (A-2)$$

with

$$\theta(t) = 0 \qquad \text{for } t<0$$
$$= 1 \qquad \text{for } t>0. \qquad (A-3)$$

It is convenient to make Fourier transformation of the susceptibility (A-2):

$$1/(2\pi)\int_{-\infty}^{\infty} d\omega\chi^{+-}(\omega)e^{i\omega t}$$

$$= [i(g\mu_B)^2/\hbar]\int_{-\infty}^{\infty} dt'\ \delta(t-t')\theta(t')\langle[S^-,S^+(t')]\rangle \equiv \phi(t). \qquad (A-4)$$

Expanding both sides of Eq. (A-4) into powers of t, we obtain

$$1/(2\pi)\int_{-\infty}^{\infty} d\omega\chi^{+-}(\omega)\sum_{n=0}^{\infty}\frac{(i\omega)^n}{n!}t^n = \sum_{n=0}^{\infty}\frac{\phi^n(+0)}{n!}t^n . \qquad (A-5)$$

Then, the zero-th and first moments are easily obtained from Eq. (A-5) as

$$\mu_0 = \int_{-\infty}^{\infty} Im\chi^{+-}(\omega)d\omega = Im\phi(+0)$$

$$= [(g\mu_B)^2/\hbar]\langle[S^-,S^+]\rangle = -[2(g\mu_B)^2/\hbar]\langle S^z\rangle \qquad \text{(A-6)}$$

and

$$\mu_1 = \int_{-\infty}^{\infty} \omega Im\chi^{+-}(\omega)d\omega = -Re\phi'(+0)$$

$$= -(g\mu_B/\hbar)^2\langle[S^-,[S^+,\mathcal{H}]]\rangle. \qquad \text{(A-7)}$$

We therefore have

$$\hbar\omega = \hbar\mu_1/\mu_0 = \langle[S^-,[S^+,\mathcal{H}]]\rangle/2\langle S^z\rangle. \qquad \text{(A-8)}$$

APPENDIX B: Derivation of Eq. (22)

For convenience we shall divide the summations $\sum_{i=0}^{N}\sum_{j=0}^{N}$ in Eq. (20) into four parts as follows:

$$\sum_{i=0}^{N}\sum_{j=0}^{N} = \sum_{i=0}^{m}\sum_{j=m+1}^{N} + \sum_{i=m+1}^{N}\sum_{j=0}^{m} + \sum_{i=0}^{m}\sum_{j=0}^{m} + \sum_{i=m+1}^{N}\sum_{j=m+1}^{N}. \qquad \text{(A-9)}$$

Each correlation function in zero field which is to be summed

in Eq. (A-9) can be written as

$$\langle s_m^{\gamma} s_{m+1}^{\gamma} s_i^{z} s_j^{z} \rangle$$

$$= Z_N^{-1} \int \frac{d\Omega_0}{4\pi} \cdots \int \frac{d\Omega_N}{4\pi} (s_m^{\gamma} s_{m+1}^{\gamma} s_i^{z} s_j^{z}) \exp(K \sum_{n=1}^{N} \vec{s}_n \vec{s}_{n-1}), \tag{A-10}$$

where $d\Omega_j$ is the element of solid angle for the vector $\vec{s}_j$ and the partition function Z_N has been given by Fisher as

$$Z_N = [(\sinh K)/K]^N. \tag{A-11}$$

To perform the integrals, we define two sets of polar angles for $\vec{s}_j$ as indicated in Fig. 9, one is a set of θ_j and ϕ_j referred to $\vec{s}_{j+1}$ (or $\vec{s}_{j-1}$) as polar axis and the other is a set of Θ_j and Φ_j referred to the z-axis. There are the following relations among these angles:

$$\cos \Theta_j = \cos \Theta_{j+1} \cos \theta_j + \sin \Theta_{j+1} \sin_j \Theta \cos \phi_j,$$

$$\sin \Theta_j \cos \Phi_j = \sin \Theta_{j+1} \cos \Phi_{j+1} \cos \theta_j$$

$$- \cos \Theta_{j+1} \cos \Phi_{j+1} \sin \theta_j \cos \phi_j$$

$$- \sin \Phi_{j+1} \sin \theta_j \sin \phi_j,$$

$$\sin \Theta_j \sin \Phi_j = \sin \Theta_{j+1} \sin \Phi_{j+1} \cos \theta_j$$

$$- \cos \Theta_{j+1} \sin \Phi_{j+1} \sin \theta_j \cos \phi_j$$

$$+ \cos \Phi_{j+1} \sin \Theta_j \sin \phi_j, \tag{A-12}$$

We shall here evaluate a fourth order spin correlation function for $j > i > m+1$ and $\gamma=z$ as an example. By Fisher's method, the integrals for $n < m$, $n > j$, $i < n \leq j$, and $n=m$ can be performed, which yield

$$[(\sinh K)/K]^{m}, \quad [(\sinh K)/K]^{N-j},$$

$$\cos \Theta_i u^{j-i}[(\sinh K)/K]^{j-i}, \text{ and } \cos \Theta_{m+1} u[(\sinh K)/K]$$

respectively. The remainder then becomes

$$[K/(\sinh K)]^{i-m-1} \int \frac{d\Omega_{m+1}}{4\pi} \cdots \int \frac{d\Omega_i}{4\pi}$$

$$\times \cos^2 \Theta_{m+1} \cos^2 \Theta_i \exp\left(\sum_{n=m+2}^{i} \vec{s}_n \cdot \vec{s}_{n-1} \right)$$

and, by using the angular relations (A-12) recurrently, reduces to

$$\langle s_m^z s_{m+1}^z s_i^z s_j^z \rangle = (1/9)u^{j-i+1}\{1 + (4/5)v^{i-m-1}\}, \qquad \text{(A-13)}$$

where v is defined by Eq. (46).

For other typical cases, only the results are presented in the following:

for $j > i > m+1$ and $\gamma=x$,

$$\langle s_m^x s_{m+1}^x s_i^z s_j^z \rangle = (1/9)u^{j-i+1}\{1 - (2/5)v^{i-m-1}\}, \qquad \text{(A-14)}$$

for $i < m$, $j > m+1$, and $\gamma=z$,

$$\langle s_m^z s_{m+1}^z s_i^z s_j^z \rangle = (1/5)u^{j-i-1}\{1 - (4/3)(u/K)\}, \qquad \text{(A-15)}$$

for $i < m$, $j > m+1$, and $\gamma = x$,

$$\langle s_m^x s_{m+1}^x s_i^z s_j^z \rangle = (1/15)u^{j-i-1}v. \qquad \text{(A-16)}$$

By summing up these results according to Eq. (A-9), we obtain Eq. (22) in the text.

APPENDIX C:

Using the Hamiltonian (19), $\langle (S_m^z)^2 - (S_m^x)^2 \rangle$ in the presence of a small external field parallel to the z-direction can be expressed in terms of the higher order spin correlation functions in zero field. To second order in H, we have

$$\langle (S_m^z)^2 - (S_m^x)^2 \rangle_{H \| z} = (1/2)\left[\frac{g\mu_B HS(S+1)}{kT}\right]^2 \times \sum_{i=0}^{N} \sum_{j=0}^{N} \langle [(s_m^z)^2 - (s_m^x)^2] s_i^z s_j^z \rangle_0. \qquad \text{(A-17)}$$

The summations in the right-hand side of Eq. (A-17) can be performed in the same way as in the case of Appendix B and result in

$$\frac{2}{15}\left\{\frac{(1+u)(1+v)}{(1-u)(1-v)} + \frac{2u}{(1-u)^2}\right\}. \qquad \text{(A-18)}$$

REFERENCES

(1) For example, H. Mori and K. Kawasaki: Progr. theor. Phys. 26 (1962) 971; H. Mori: ibid. 33 (1965) 399; H. Mori: symposium on Inelastic Scattering Neutrons by Condensed systems, Brookhaven National Laboratry (1965) 940 (C-45); H. Mori: Tokyo Summer Lectures in Theoretical Physics, Part 1 (1966) 17.

(2) For example, M. S. Seehra: J. appl. Phys. 42 (1971) 1290; K. Nagata and M. Date: J. Phys. Soc. Japan 19 (1964) 1823; E. Toyota and K. Hirakawa: ibid. 29 (1970) 1093.

(3) D. H. Douglass and M. W. P. Strandberg: Physica 27 (1961) 1.

(4) M. P. Petrov and S. A. Kizhaev: Soviet Physics-Solid State 11 (1970) 1968.

(5) Y. Tazuke and K. Nagata: J. Phys. Soc. Japan 30 (1971) 285.

(6) Y. Morimoto and M. Date: J. Phys. Soc. Japan 29 (1970) 1093.

(7) M. E. Fisher: Am. J. Phys. 32 (1964) 343.

(8) T. Smith and S. A. Friedberg: Phys. Rev. 176 (1968) 660; H. Kobayashi and S. A. Friedberg: private communication

(9) R. J. Birgeneau, R. Dingle, M. T. Hutchings, G. Shirane, and S. L. Holt: Phys. Rev. Letters 26 (1971) 718.

(10) S. J. Jensen, P. Andersen and S. E. Rasmussen: Acta chem. Scand. 16 (1962) 1890.

(11) B. Morosin and E. J. Graever: Acta cryst. 23 (1967) 766.

(12) J. Skalyo, G. Shirane, S. A. Friedberg, and H. Kobayashi:

Phys. Rev. B2 (1970) 1310, B2 (1970) 4632.

(13) R. Dingle, M. E. Lines, and S. L. Holt: Phys. Rev. 187 (1969) 643.

(14) F. Bloch: Phys. Rev. 70 (1946) 460.

(15) J. Kanamori and M. Tachiki: J. Phys. Soc. Japan 17 (1962) 1384.

(16) R. D. Spence, J. A. Casey, and V. Nogarajen: J. appl. Phys. 39 (1968) 1011.

(17) K. Nagata and Y. Tazuke: Phys. Letters 31A (1970) 923.

(18) R. D. Spence, W. J. M. de Jonge, and K. V. S. Rama Rao: J. chem. Phys. 51 (1969) 4694.

(19) G. J. Butterworth and J. A. Woolam: Phys. Letters 29A (1969) 259.

(20) A. C. Botterman, W. J. M. de Jonge, and P. de Leeuw: Phys. Letters 30A (1969) 150.

(21) K. E. Lawson: J. chem. Phys. 47 (1967) 3627.

FIGURE CAPTIONS

Fig. 1(a) Behavior of the function F(x).

Fig. 1(b) Behavior of the function P(x).

Fig. 2(a) Behavior of the function G(x).

Fig. 2(b) Behavior of the function Q(x).

Fig. 3 Projection of half of the unit cell of $CsMnCl_3 2H_2O$ on the c-plane.

Fig. 4(a) Projection of a unit cell of TMMC on the c-plane. $-MnCl_3^-$- chains extend infinitely along the c-axis. $[N(CH_3)_4]^+$ ions are located between these chains in a highly disordered manner. Mn^{2+} positions are (000) and (001/2).

Fig. 4(b) A sketch of the $-MnCl_3^-$- chain found in TMMC. The octahedral environment about the Mn^{2+} ion is slightly distorted, corresponding to a lengthening along the chain.

Fig. 5 Comparison of theory with experiment in the shift of resonance field in $CsMnCl_3 2H_2O$ at 34.4 GHz in the temperature range up to 70 K. Measured values of the shift are indicated by +(H∥a), ○(H∥b) and ◉(H∥c). The solid curves are computed with Eq. (24) and (25) of the text. The high temperature g-value is 2.000.

Fig. 6 Comparison of theory with experiment in the shift of resonance field in TMMC at 34.9 GHz in the tempera-

ture range up to 100 K. Measured values of the shift are indicated by +(H∥c) and o(H⊥c). The solid curves are computed with Eq. (24) and (25) of the text. The dotted curves are the theoretical results with the correction of the D-term. The dashed line represents the DPPH-position. The high temperature g-value is 2.005.

Fig. 7 Measured magnetic anisotropy of $CsMnCl_3 2H_2O$.

Fig. 8 Comparison of theory with experiment on the uniaxial anisotropy of $CsMnCl_3 2H_2O$. The solid curve is computed with Eq. (32) of the text.

Fig. 9 Definition of the two sets of polar angles for $\vec{s}_j$ referred to $\vec{s}_{j+1}$ and the z-direction.

Fig. 1

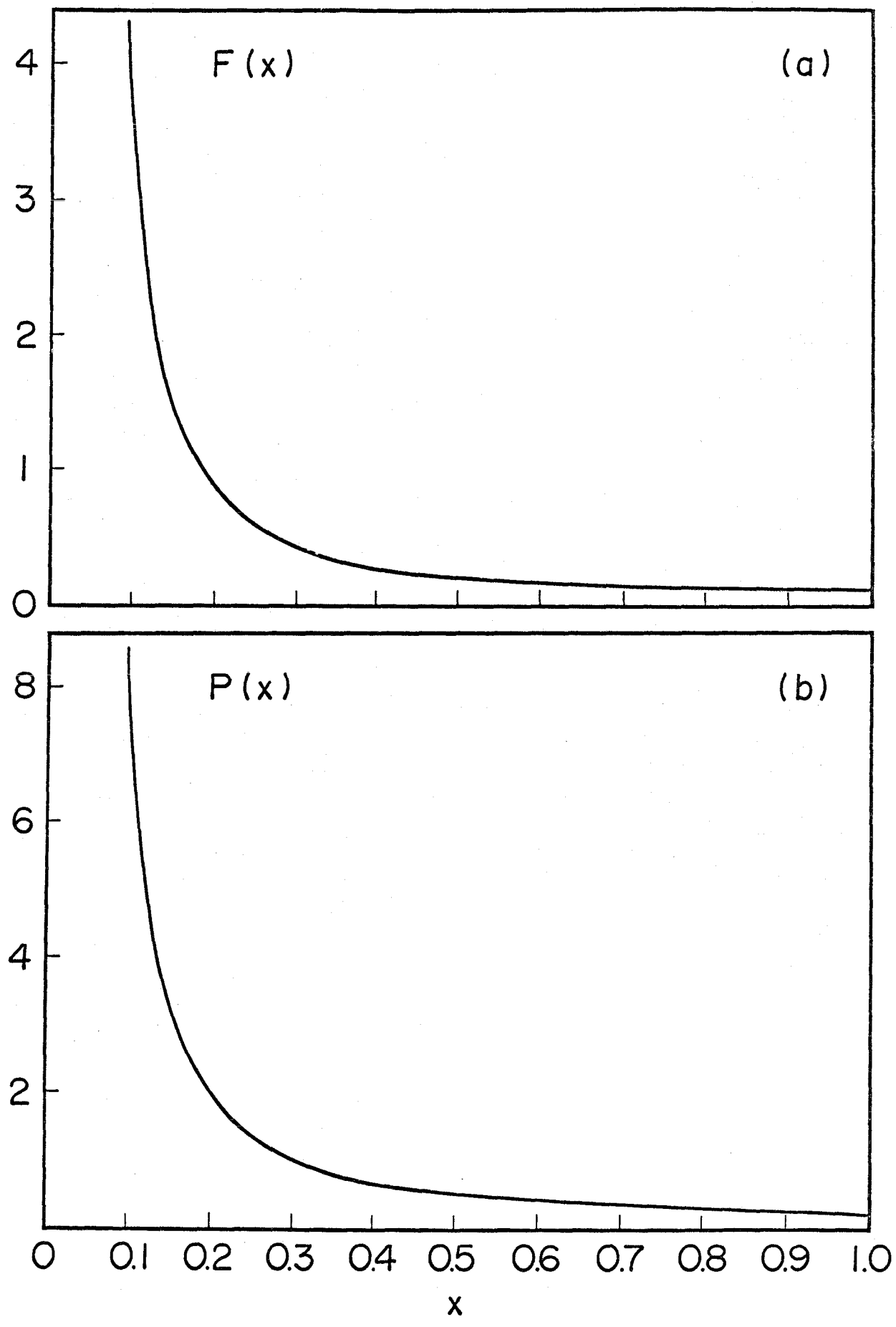

Fig. 2

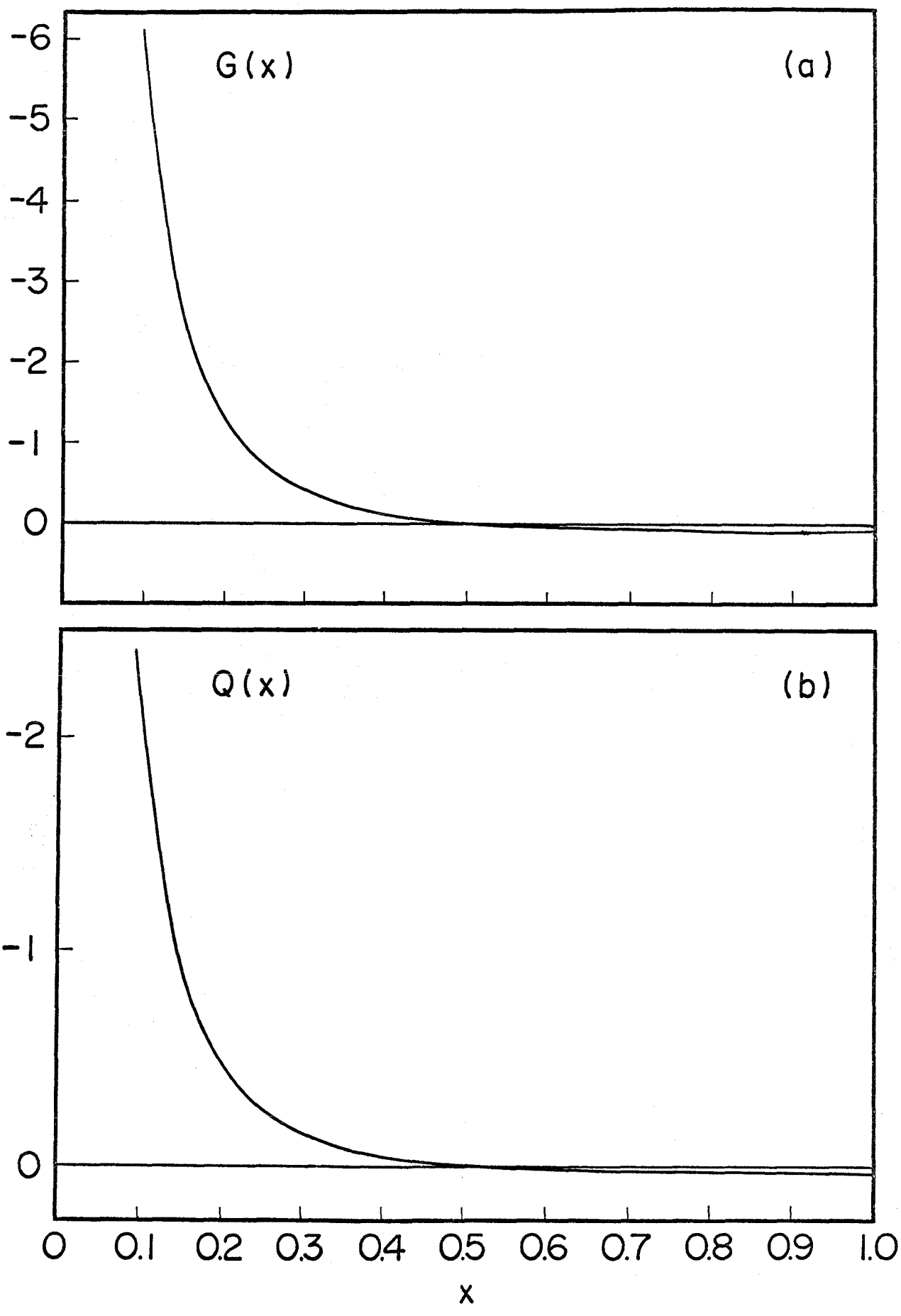

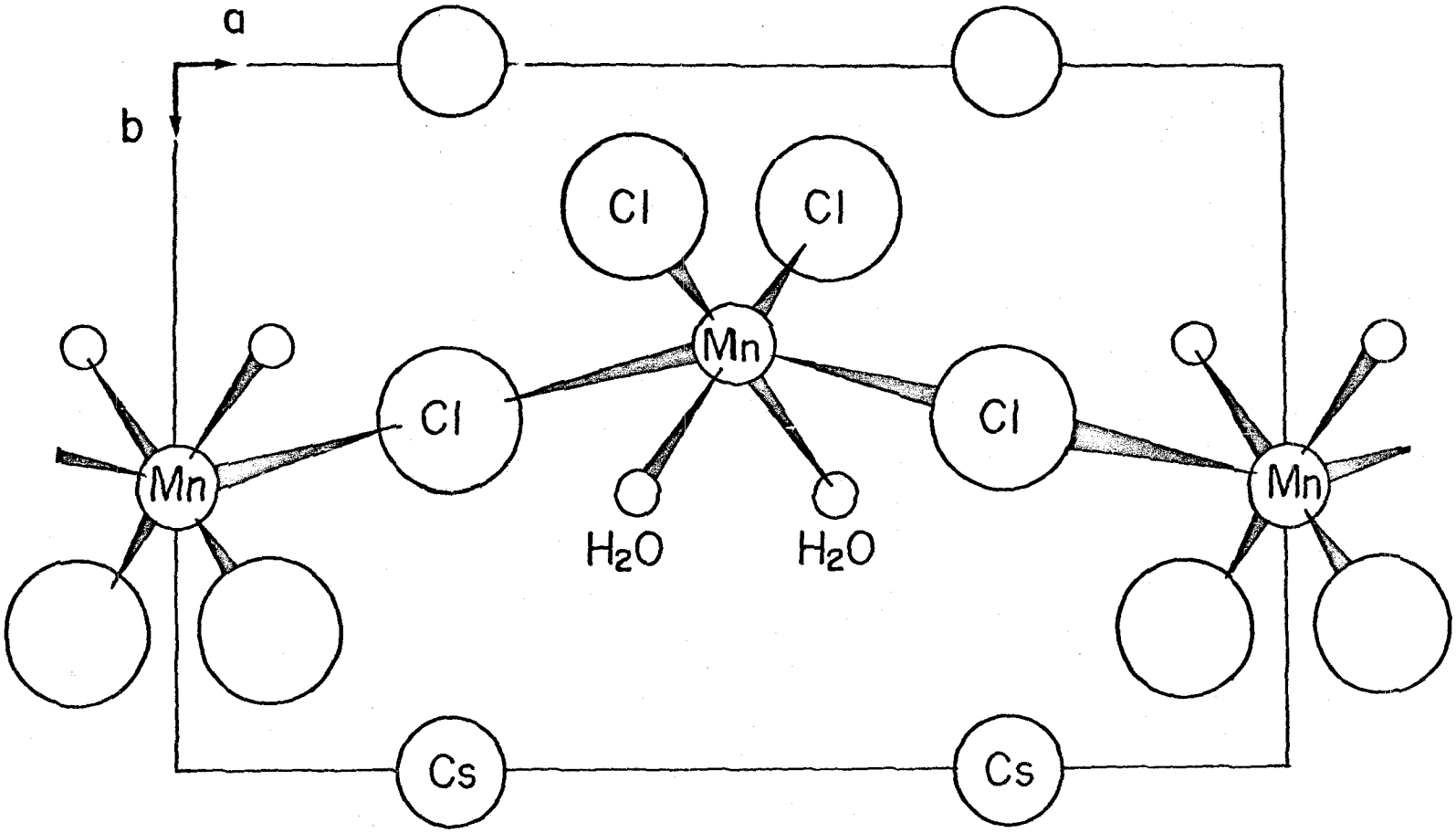
a
b
Cl
Cl
Mn
Cl
Cl
Mn
Mn
H_2O
H_2O
Cs
Cs

Fig. 4(a)

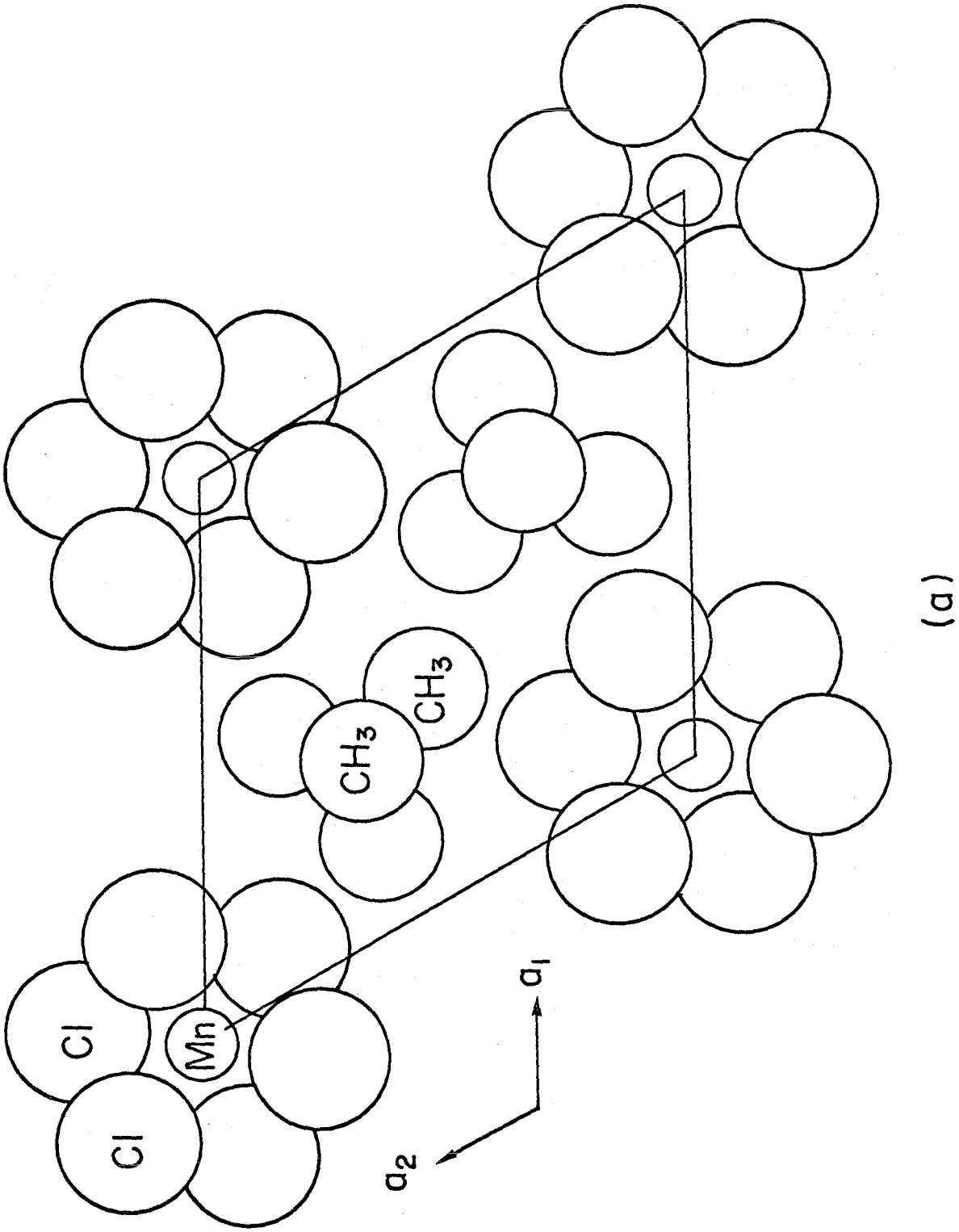

Fig. 4(b)

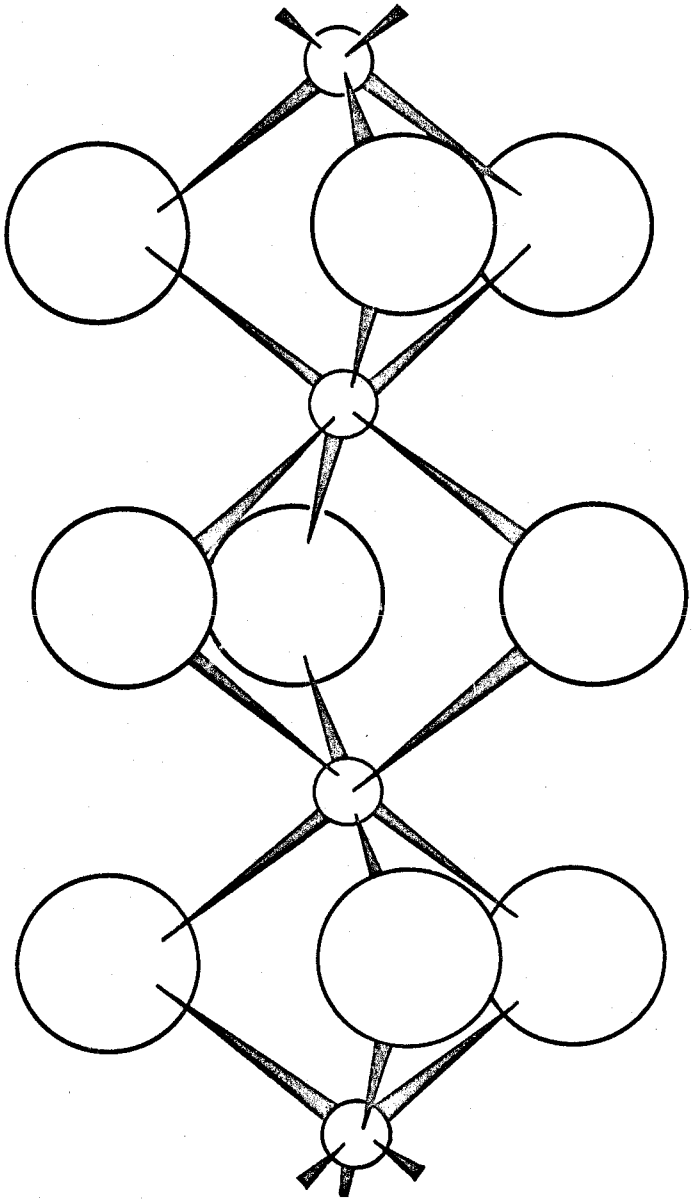

(b)

Fig. 5

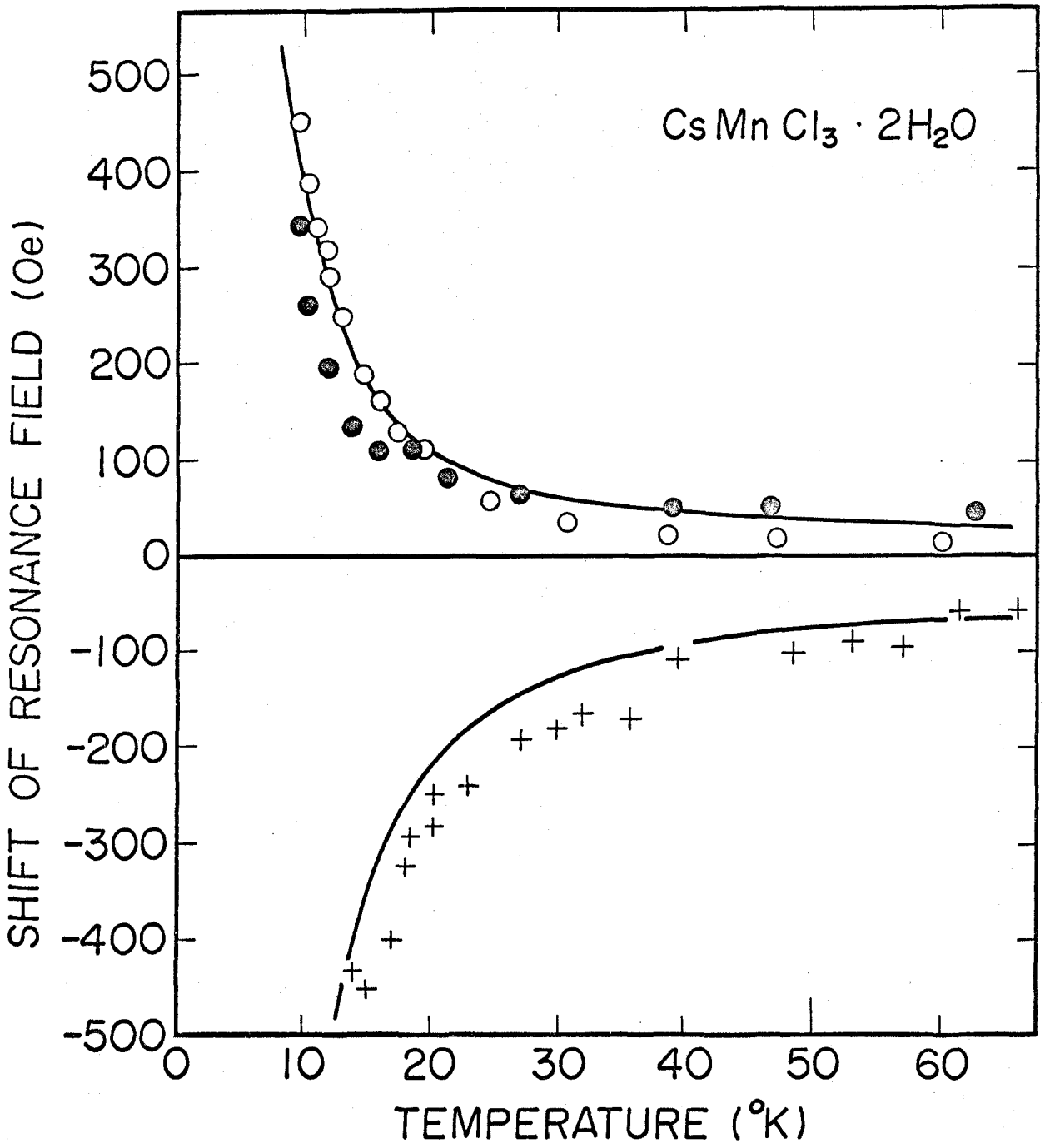
Cs Mn Cl3 · 2H2O
SHIFT OF RESONANCE FIELD (Oe)
500
400
300
200
100
0
-100
-200
-300
-400
-500
0
10
20
30
40
50
60
TEMPERATURE (°K)

Fig. 6

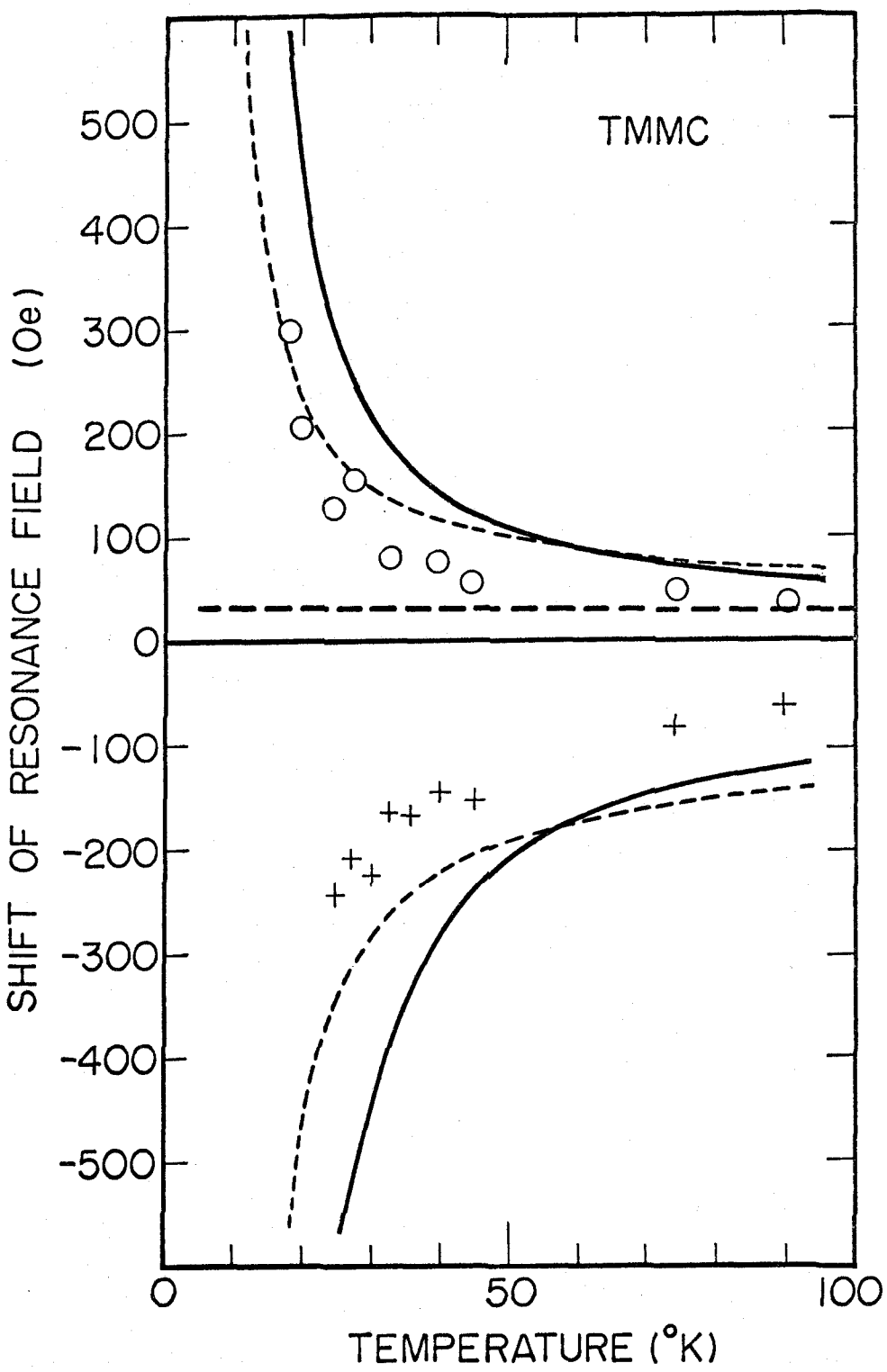
TMMC
500
400
300
200
100
0
-100
-200
-300
-400
-500
SHIFT OF RESONANCE FIELD (Oe)
0
50
100
TEMPERATURE (°K)

Fig. 7

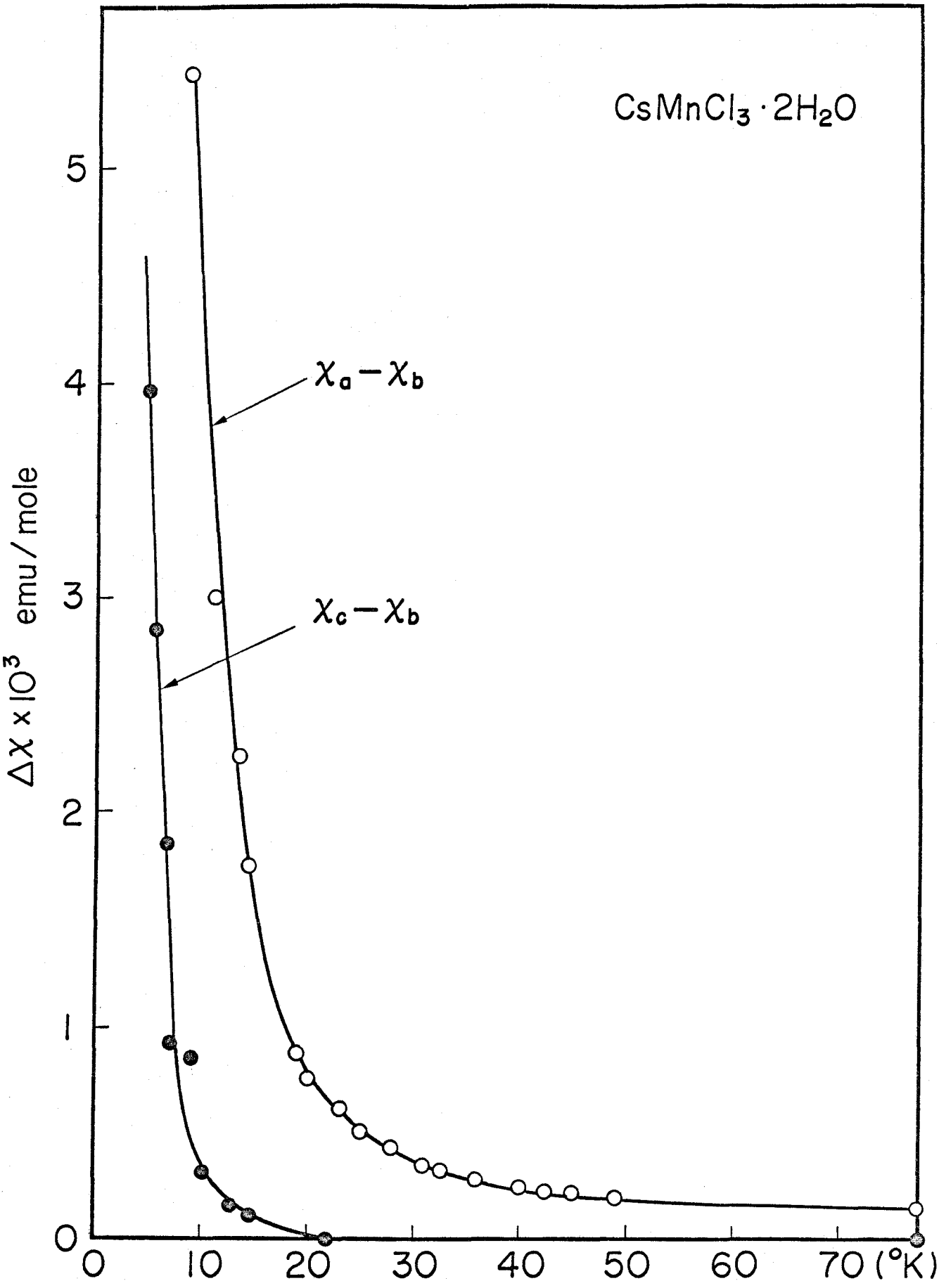
CsMnCl3 · 2H2O
χa − χb
χc − χb
Δχ x 10³ emu/mole
0
1
2
3
4
5
0
10
20
30
40
50
60
70 (°K)

Fig. 8

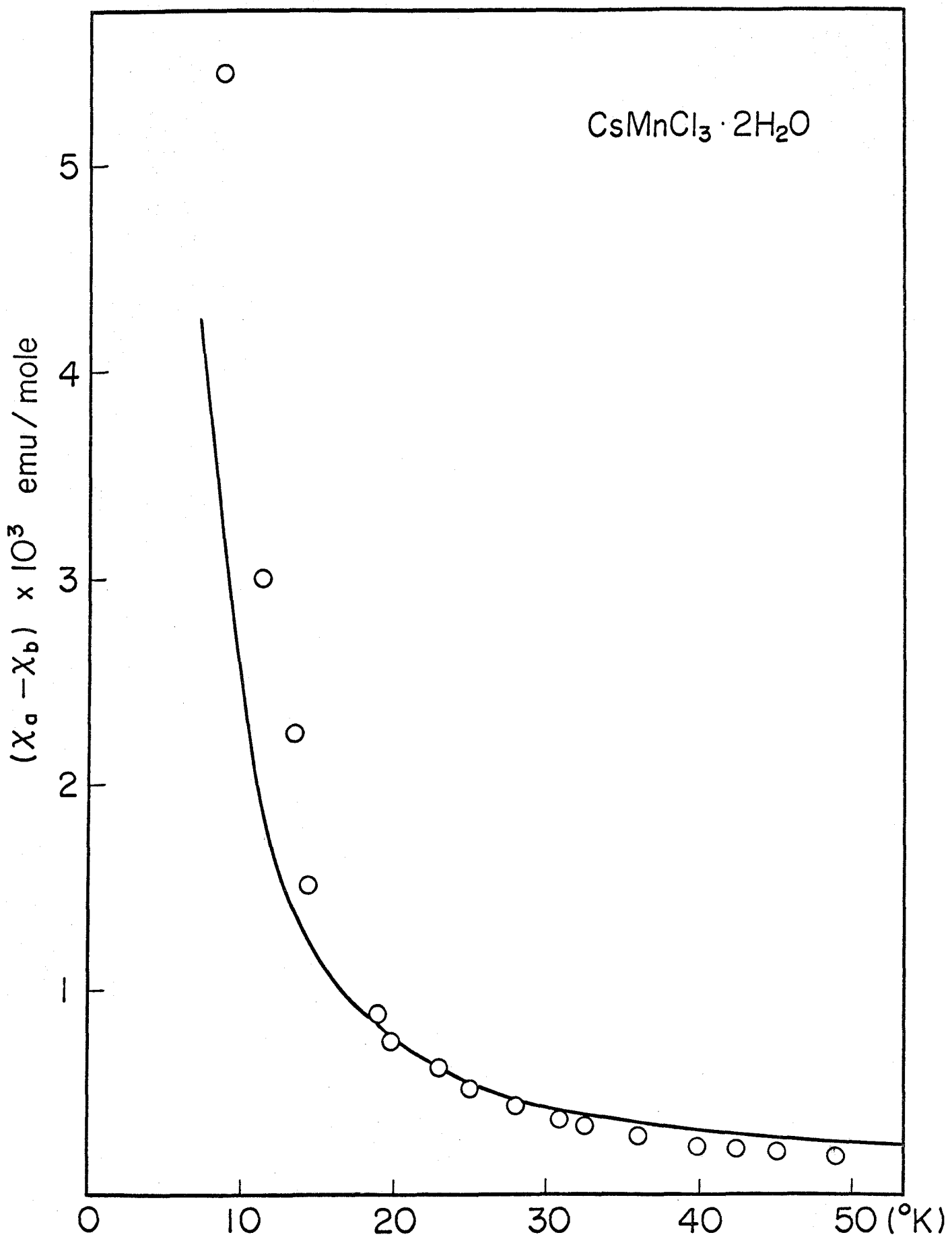
$CsMnCl_3 \cdot 2H_2O$
$(\chi_a - \chi_b) \times 10^3$ emu/mole
5
4
3
2
1
0
10
20
30
40
50 (°K)

Fig. 9